SCIENTIFIC PAPERS
OF THE UNIVERSITY OF PARDUBICE
Series A
Faculty of Chemical Technology
15 (2009)

USABILITY OF $NaNO_2$ FOR LATENT HEAT STORAGE APPLICATIONS

Lucie ORAVOVÁ[1a] and Roman SVOBODA[b]
[a]Department of Inorganic Technology,
[b]Department of Physical Chemistry
The University of Pardubice, CZ–532 10 Pardubice

Received September 30, 2009

Enthalpy of fusion and heat capacity of $NaNO_2$ were determined. The heat capacity measurements were performed in the temperature range 0-310 °C by using two types of calorimeters. Melting point of $NaNO_2$ was detected at 280.7 ± 0.2 °C and the corresponding heat of fusion was found to be 13.9 ± 0.2 kJ mol^{-1}. Thermal stability of the studied material was first investigated using simultaneous TG-DTA and was followed by DSC accelerated thermal cycle tests. During these tests, 300 heating/cooling thermal cycles were performed through the melting region of $NaNO_2$ — enthalpies; onset and peak temperatures of fusion and crystallization were determined from these measurements.

[1] To whom correspondence should be addressed.

Introduction

Thermal energy can be stored and released in many different ways, e.g. during chemical reaction, during physical adsorption, etc. However, one of the most efficient ways of storing thermal energy is the latent heat storage [1]. In latent heat storage (LHS) applications the thermal energy is stored and released whenever the storage material undergoes a phase change. Nowadays, the most frequently exploited phase changes are the solid-solid (between different modifications) and solid-liquid (melting, crystallization) transitions. The main advantages of the phase change materials (PCMs) utilization are their high energy storage density and the possibility of storing energy also during isothermal and quasi-isothermal operations. Knowledge of heat capacity and enthalpy change during the considered transition is then necessary for the calculation of the energy amount that can be stored in the substance. The storage capacity of the LHS system with PCM medium is given (considering a change from solid to liquid phase) by the following equation

$$Q = m\int_{T_i}^{T_m} c_{p(s)}(T)\,\mathrm{d}T + \Delta_f H + \int_{T_m}^{T_f} c_{p(l)}(T)\,\mathrm{d}T \qquad (1)$$

where $c_{p(s)}$ and $c_{p(l)}$ (in J g^{-1} K^{-1}) are heat capacities of solid and liquid phase, respectively, $\Delta_f H$ (in J g^{-1}) is the enthalpy of fusion, T_m (in K) is temperature of the phase change (melting in this case) and m (in g) is total mass of the material. Besides the desired high values of heat capacity and enthalpy change during the transition, also several other parameters have to be taken into account for the heat storage applications — i.e. suitable temperature range of the phase transition, high thermal conductivity, low reactivity, price of the material and very importantly the stability of PCM during the accelerated thermal cycle tests. Accelerated thermal cycle test consists of a number of alternating heating and cooling cycles performed in a laboratory, during which real conditions are simulated and during which no supercooling or degradation is allowed to occur.

Sodium nitrite belongs to a group of phase change materials and as such it might find utilization in high temperature range energy storage applications (e.g. in solar power plants). $NaNO_2$ melts at approximately 280 °C [2-4], while other two phase transitions can be found in solid state near 164 °C [5-11]. These two additional transitions are associated with closely following changes between the ferroelectric phase, sinusoidal antiferroelectric phase and paraelectric phase.

Heat capacity and enthalpy of phase transitions were for $NaNO_2$ reported by Sakiyama and co-workers [5] in the temperature range of 2-195 °C. Similar heat capacity measurements were carried out by Hoshino [12] in the narrow temperature interval near the two solid-solid transitions. Heat capacity in the

temperature range of 27-202 °C with an emphasis on the solid-solid transitions region is published in the papers of Hatta *et al.* [10-11]. In the work of Kamimoto [2] and Cases [3], calorimetric measurements were performed to determine the heat of fusion and heat capacity of liquid $NaNO_2$. Both solid-solid transitions have been also studied by using various other experimental techniques: X-ray diffraction [13-15], spectroscopic methods [8,16-18], dielectric measurements [9,19-21].

The aim of this work was to investigate whether $NaNO_2$ might be a suitable material for LHS applications. In the first part of the paper the enthalpy of fusion as well as the heat capacity of $NaNO_2$ (from 0 °C up to the melting temperature of the sample) are determined. In the second part of the paper the thermal stability of $NaNO_2$ is studied by means of the accelerated thermal cycle test — 300 cycles were performed.

Experimental

$NaNO_2$ and Its Characterization

The sodium nitrite sample used in this work was of analytical reagent grade ($NaNO_2$ content ~ 99.8 %). The sample was oven-dried at the temperature of 120 °C for 24h and stored in a desiccator. X-Ray diffraction data of the sample were obtained at the temperature of 25 °C for CuKα radiation by using the D8-Advance diffractometer (Bruker AXE, Germany) and secondary graphite monochromator The X-ray diffraction confirmed orthorhombic, body-centred lattice with the parameters $a = 3.5726 \pm 0.0010$ Å, $b = 5.5835 \pm 0.0012$ Å and $c = 5.4015 \pm 0.0012$ Å. The lattice parameters are in a good agreement with published data [22]. In addition, a combined TG-DTA measurement of $NaNO_2$ was performed by using STA Jupiter 449/C/6/F (Netzsch, SRN). The measurement was performed at the speed of 10 °C min^{-1} in the temperature range of 100-600 °C and is shown in Fig. 1. The decrease in TG curve corresponding to the loss of the sample mass is apparent to begin at the temperature of approximately 435 °C i.e. ~170 °C above the melting point.

Methods of Measurement

DSC Pyris 1 (Perkin-Elmer, USA) and C80 calorimeter (Setaram, France) were used for the experimental measurements. Heat capacity and enthalpy of fusion were measured by means of the DSC Pyris 1 in the temperature range of 0-310 °C. Melting temperatures of pure metals (Hg, Ga, In, Sn, Pb) and enthalpy of fusion of In were used to calibrate the calorimeter. The sample masses were approximately 10 mg. All the measurements were performed under the dry nitro-

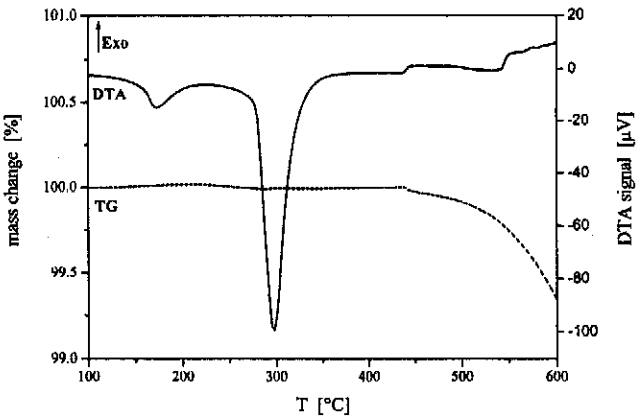

Fig. 1 Combined DTA-TG measurement of the $NaNO_2$ sample

gen atmosphere (20 cm^3 min^{-1}). The heat capacity was determined from the measurements by the so called ratio method [23]; this procedure required one additional measurement with a standard material (sapphire in our case) at the same heating rate as was that of the original sample measurement. Accuracy of the heat capacity measurements was tested by measuring molybdenum (NIST Standard reference material No. 781D2) in the temperature range of 20-300 °C. The accuracy for the DSC Pyris 1 was estimated to be better than 2 %. The precision of heat capacity measurements was determined from five reproduced curves and was found to be better than ± 2.5 %. The long term stability of $NaNO_2$ was tested by means of the accelerated thermal cycle test using 300 thermal cycle. Each cycle consisted of three steps — first a heating step was performed at the speed of 20 °C min^{-1} from the temperature of 25 to 315 °C, then a 5 minutes isothermal step followed and lastly the sample was cooled at the speed of 20 °C min^{-1} from the temperature of 315 to 25 °C. In addition, every tenth cycle was performed at heating and cooling rates equal to 5 °C min^{-1} (instead of 20 °C min^{-1}) in order to obtain a better resolution on the temperature axis for the investigated thermal effects.

Additional heat capacity measurements were done using the C80 heat conduction differential calorimeter. The measurement temperature range is limited for this device to the 30-290 °C interval. The sample mass was approximately 7 g. The calorimeter was calibrated electrically using the Joule-effect calibration unit supplied by Setaram. The heat capacity was determined by the thermal increment method. Details of the method are described elsewhere [17]. The synthetic sapphire, NIST Standard reference material No. 720, was used as the reference material. The accuracy of heat capacity measurements was found to be better than 3 %. The heat capacity measurements were repeated three times with the standard deviation better than 2 %.

Results and Discussion

Heat Capacity and Enthalpy of Fusion

The experimental values of molar heat capacity obtained for $NaNO_2$ from the DSC Pyris 1 and C80 measurements are presented in Table I (the introduced DSC data were acquired at the heating rate of 5 °C min^{-1}, the heat capacity data are given in units J mol^{-1} K^{-1}). These data are shown in Fig. 2 together with the values obtained by Sakiyama *et al.* [5].

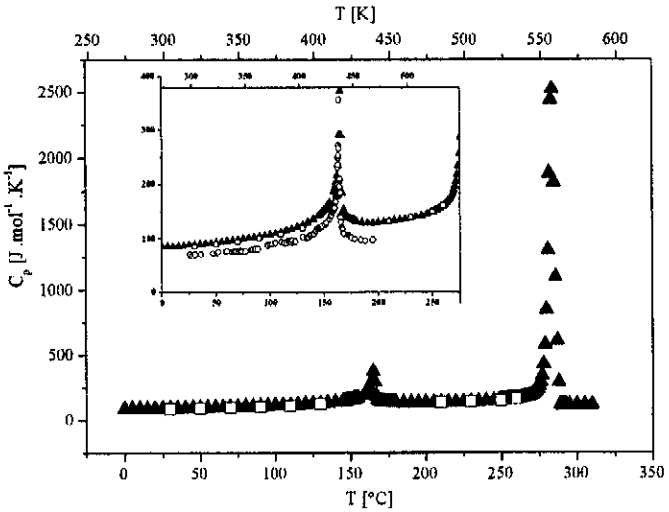

Fig. 2 Heat capacity of $NaNO_2$: ▲ DSC Pyris 1; □ Setaram C80; ○ Ref. [5]; heating rate 5 °C min^{-1}. The inset shows the heat capacity data zoomed in the solid state region

The maximum difference between the C_p values obtained by DSC and C80 was observed at the temperature of 130 °C, where the C80 values were by approximately 4 % lower than those obtained by DSC. Origin of this divergence may lie in the fact that different methods of C_p evaluation (ratio vs. increment) and different sample masses (masses in the order of few milligrams in the case of DSC vs. several grams of sample in the case of C80) were used in each case. However, the precision envelopes of heat capacity measurements performed by means of both instruments at least partially superpose, thus the difference lies within the statistical error. If we compare our data to those of Sakiyama, one can see that his C_p values are approximately 15-19 % lower than our data. The reason for this is unknown to us so far. The heat capacity data obtained by AC calorimetry and published by Hatta *et al.* [10] are not shown in Fig. 2 because no discrete C_p values are given in that paper (only the overall C_p-T curve is shown in [10]). These data

Table I Heat capacity of $NaNO_2$ measured by the DSC Pyris 1 and Setaram C80 calorimeters

T °C	T K	C_p J mol^{-1} K^{-1}	T °C	T K	C_p J mol^{-1} K^{-1}	T °C	T K	C_p J mol^{-1} K^{-1}
0	273.15	85.2	159	432.15	186.4	256	529.15	155.0
5	278.15	85.3	160	433.15	193.9	257	530.15	156.0
10	283.15	86.0	161	434.15	203.4	258	531.15	157.5
15	288.15	86.6	162	435.15	215.9	259	532.15	158.7
20			163			260	533.15	160.2
	293.15	87.3		436.15	235.0			(161.2±2.1*)
25	298.15	88.1	164	437.15	291.1	261	534.15	161.8
30	303.15	88.8	165	438.15	372.1	262	535.15	163.1
		(85.3±0.7*)						
35	308.15	90.1	166	439.15	290.0	263	536.15	165.7
40	313.15	90.8	167	440.15	184.1	264	537.15	168.0
45	318.15	91.8	168	441.15	153.8	265	538.15	169.8
50	323.15	92.8	169	442.15	146.0	266	539.15	173.2
		(89.3±0.7*)						
55	328.15	94.0	170	443.15	142.7	267	540.15	176.4
60	333.15	95.3	171	444.15	140.5	268	541.15	180.0
65	338.15	96.7	172	445.15	138.9	269	542.15	183.0
70	343.15	98.0	173	446.15	137.7	270	543.15	189.2
		(94.1±0.5*)						
75	348.15	99.8	174	447.15	136.7	271	544.15	196.3
80	353.15	101.3	175	448.15	136.1	272	545.15	205.3
85	358.15	102.5	176	449.15	135.4	273	546.15	217.8
90	363.15	103.5	177	450.15	134.8	274	547.15	234.2
		(99.9±2.0*)						
95	368.15	106.2	178	451.15	133.3	275	548.15	256.4
100	373.15	108.2	179	452.15	132.5	276	549.15	286.8
105	378.15	109.9	180	453.15	131.4	277	550.15	337.5
110	383.15	111.6	185	458.15	129.8	278	551.15	425.6
		(107.8±0.7*)						
115	388.15	115.3	190	463.15	128.9	279	552.15	578.4
120	393.15	118.2	195	468.15	129.0	280	553.15	846.7
125	398.15	121.5	200	473.15	129.8	281	554.15	1304.6
130	403.15	124.4	205	478.15	130.8	282	555.15	1880.7
		(119.3±0.8*)						
135	408.15	130.0	210	483.15	131.9	283	556.15	2436.9
					(131.6±1.5*)			
140	413.15	135.6	215	488.15	133.2	284	557.15	2519.7
145	418.15	142.7	220	493.15	134.7	285	558.15	1810.3
146	419.15	144.4	225	498.15	136.0	286	559.15	1098
147	420.15	146.2	230	503.15	137.8	287	560.15	611.3
					(138.7±0.7*)			
148	421.15	148.1	235	508.15	140.0	288	561.15	287.2
149	422.15	150.1	240	513.15	142.4	289	562.15	116.8
150	423.15	152.4	245	518.15	145.2	290	563.15	110.0
151	424.15	154.7	248	521.15	147.7	291	564.15	110.2
152	425.15	157.3	249	522.15	148.5	292	565.15	109.9
153	426.15	160.3	250	523.15	148.9	293	566.15	110.2
					(148.8±2.4*)			
154	427.15	163.3	251	524.15	149.8	295	568.15	110.9
155	428.15	166.7	252	525.15	150.9	300	573.15	111.9
156	429.15	170.6	253	526.15	152.0	305	578.15	112.3
157	430.15	175.1	254	527.15	153.0	310	583.15	112.6
158	431.15	180.4	255	528.15	153.2		-	-

* Setaran C80 measurements

were again published by Hatta in [11] but already after a correction. According to what is described in [11] this correcting procedure is a form of correction applied by Hatta to his own older data due to the exclusion of additional heat capacity associated with the thermocouple and glue attached to the sample during ACC measurements. However, after digitizing the data from Fig. 3 in [11] we could see that the C_p data published by Hatta are in a good agreement with our values. The difference between the two dependencies was approximately 2 % (Hatta's data being lower). The experimental molar heat capacities obtained by DSC were fitted using a polynomial function (Eq. (2)). This was done within two separate temperature regions (due to the presence of the two solid-solid phase transitions), the first temperature range being 0-135 °C (273.15-408.15 K) and the second 190-257 °C (463.15-530.15 K). These temperature regions were chosen to be the widest possible while still having the correlation coefficient of the resulting fit $R^2 \approx 0.995$. Final parameters of both polynomial equations are listed in Table II (the confidence intervals were calculated as ± 1 σ).

$$C_p = P_1 + P_2 T + P_3 T^2 \tag{2}$$

Table II Parameters (P_1, P_2, P_3) and coefficient of determination (R^2) of the polynomial function (2) used to fit the heat capacity data

Parameter	Temperature interval, K	
	273.15-408.15	463.15-530.15
P_1	237 ± 15	1469 ± 97
P_2	−1.128 ± 0.086	−5.75 ± 0.39
P_3	(2.10 ± 0.12)×10^{-3}	(6.17± 0.39) ×10^{-3}
R^2	0.9947	0.9959

The melting point investigated by the DSC was detected at 280.7 ± 0.2 °C and the corresponding heat of fusion was 13.94 ± 0.21 kJ mol^{-1}. These results are close to the values 15.3 kJ mol^{-1} published by Kamimoto [2] and 14.9 ± 0.8 kJ mol^{-1} introduced by Cases [3].

From the results introduced in this chapter (relatively high values of heat capacity and heat of fusion) it is apparent that $NaNO_2$ so far seems to be a promising material for LHS applications.

Thermal Cycle Tests

In order to be used in LHS applications the material has to have not only high values of C_p and $\Delta_f H$ but it also has to be thermally stable. In other words, the values of C_p and $\Delta_f H$ should not change over the time of material's utilization, no decomposition or other degradation processes should occur during the material's usage life-time. This requirement is usually tested in the so called accelerated thermal cycle test. In our study we performed several sets of these tests in order to determine whether and under which conditions $NaNO_2$ could be used in LHS applications. It is known that sodium nitrite starts to decompose at the temperature of approximately 320 °C to give nitrogen gas and sodium oxide [24-26]. Moreover, it can be seen from our TG-DTA sample characterization measurement (Fig. 1) that the substance actually started to decompose at the temperature of approximately 440 °C, which is much higher than the decomposition temperature previously reported. However, the sensitivity of TG-DTA measurements to detect first traces of nitrite decomposition may probably be not as high as, e.g., that of gas analysis measurements reported in literature [24,25]. Nevertheless, even the decomposition temperature equal to 320 °C theoretically gives a large enough temperature region between the melting and decomposition processes to safely operate with $NaNO_2$ in any LHS application. The question is whether this will be also true during repeated subjecting of the material to thermal stresses.

In our first testing set of cycles the conditions were exactly as described in the chapter Methods of Measurement — the upper temperature was for all the cycles set to be 315 °C (that is 5 °C below the published decomposition temperature). Rather qualitative description of the $NaNO_2$ decomposition during the 300 performed cycles is shown in Fig. 3. In the figure the DSC curves are plotted and zoomed for every 60th cycle and both applied heating rates; the curves were shifted along the y-axis for better transparency. The proceeding decomposition is displayed as a low-temperature shoulder of the melting peak. First traces of the decomposition shoulder were observed during approximately 140th cycle for both applied heating rates. This number is very low for the substance to be used in LHS applications (usually at least 1000 cycles without a trace of degradation are required). There are two possible reasons why the sample started to decompose (though slowly) below its decomposition temperature — the repeated thermal stress might have resulted in local overheating to temperatures well above the decomposition temperature and secondly the impurities in the sample might have influenced and speeded up the rate of decomposition. The latter influence was tested in our second set of thermal cycles. The conditions were again similar to those described in the chapter Methods of Measurement — the upper temperature was for all the cycles again set to be 315 °C. The difference was only in the sample purity; in this second set of cycles the sample with very high purity (5N) was used, though it would be extremely expensive and probably also

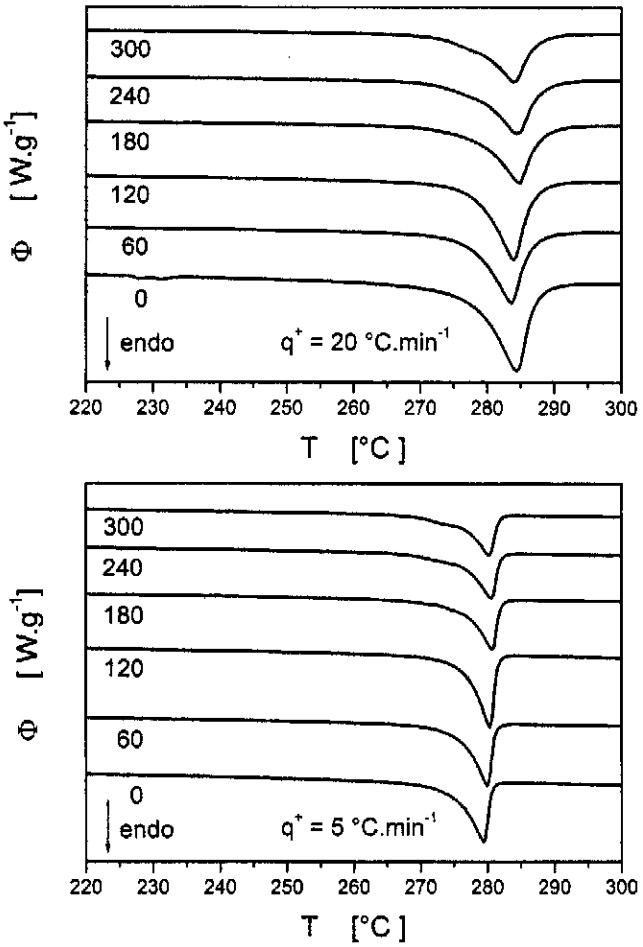

Fig. 3 First set of thermal cycles performed by using DSC Pyris 1 for $NaNO_2$ sample. See text for details

technically very difficult to use as a LHS medium in practice while keeping it constantly pure. The results are shown in Fig. 4, the DSC curves are here plotted and zoomed for every 40th cycle out of the first 200 performed, again for both performed heating rates.

In the case of this highly pure sample the first traces of the decomposition shoulder (which later turned into a separate peak) were observed during cca 100th cycle for both applied heating rates. Although it seems at first sight that the decomposition was even faster for the highly pure sample, this was probably caused by better separation of both peaks. Impurities present in the sample shift and broaden the melting peak which in the case of our former "impure" sample probably masked the early stage of decomposition. Thus it could be concluded that

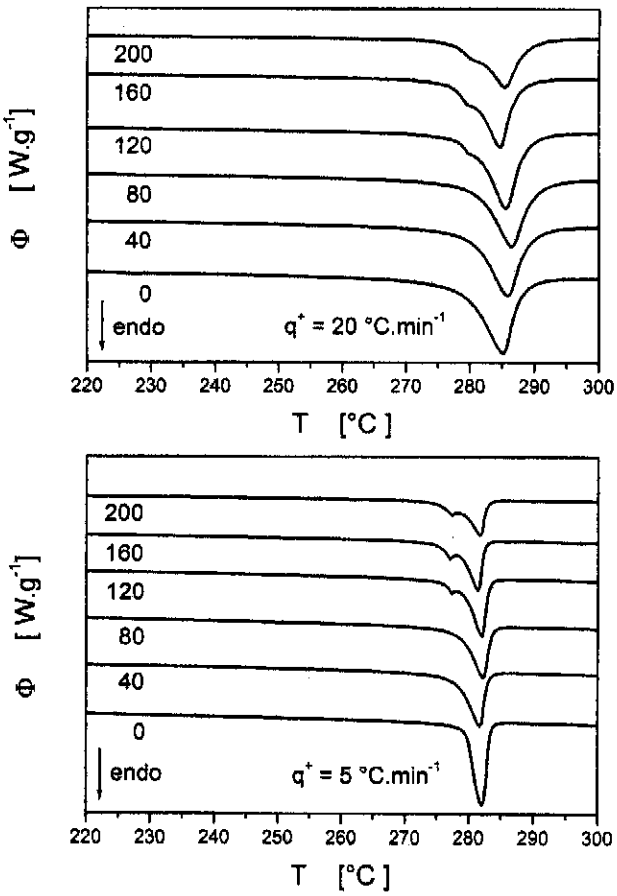

Fig. 4 Second set of thermal cycles performed by using DSC Pyris 1 for $NaNO_2$ sample. See text for details

at these temperatures the impurities present in the 99.8 %-pure sample do not influence the decomposition rate significantly. In the light of these facts the only solution how to suppress the ongoing decomposition was to significantly lower the highest temperature reached during the cycles.

Therefore, the third set of thermal cycles was performed in the temperature range of 25-295 °C. The other conditions were similar as in the case of the first and second cycle sets, the sample with purity 99.8 % was used again as this purity is probably closer to that of the material that would be used in practice in real devices. During the 300 thermal cycles performed only a very little decomposition shoulder occurred (with the area corresponding to less than 1 % of the total area under the melting peak) that would not be visible in a figure similar to Fig. 3 or Fig. 4. However, the first traces of the shoulder appeared again during cca the 130^{th} cycle for both applied heating rates. This leads to the conclusion that the

decomposition proceeds at temperatures below 320 °C; however, the process is probably strongly thermally activated as the lowered temperature during the third set of thermal cycles heavily suppressed the progression of decomposition.

Nonetheless, an accurate quantification of the degree of proceeding decomposition seems to be quite difficult using a standard DSC technique. The probably only reliable semi-quantitative method would be to estimate the area under the melting peak that corresponds to the decomposition shoulder. Reason for the difficult quantification was the sample slowly diffusing through the walls or the cold weld of the standard aluminium pan. Therefore the overall enthalpies of fusion and crystallization also slowly decreased — this decrease was similar for all thermal cycle sets performed, which kind of confirms that the rate of decomposition was not affected by this diffusion. In addition, we evaluated onsets and maxima of the melting and crystallization peaks for all three thermal cycle sets performed. The following could be concluded from the dependences: the scatter in data was significantly higher during the first 50 or 100 cycles until the sample settled; after this period the onset and maximum of the crystallization peak were oscillating around some mean value, whereas the onset and maximum of the melting peak slowly and constantly increased. This increase was, after some hundreds of cycles, decelerated by the proceeding decomposition and turned into a very slow decrease — in the case of the third set of thermal cycles where the decomposition proceeded only very slowly, the onset and maximum of the melting peak increased continually within the duration of all 300 cycles.

Conclusion

Phase change materials, which easily undergo cyclic phase changes such as alternating melting and crystallization, are desirable for thermal energy storage applications. Sodium nitrite, which melts at the temperature of 280 °C, is considered to be one of these materials. Its usage as PCM would be in higher temperature range applications e.g. as a storage material in solar power plants. A suitable phase change temperature, large melting enthalpy and large heat capacity are the three obvious requirements for the PCMs. Temperature dependence of heat capacity and enthalpy of fusion are necessary for the calculation of energy stored in the compound during heating. Heat capacity in solid state was for the sodium nitrite ($NaNO_2$) measured by using two types of calorimeters. The measurements were performed in the temperature range of 0-310 °C. Temperature of melting was determined to be 280.7 ± 0.2 °C with the corresponding heat of fusion being equal to 13.9 ± 0.2 kJ mol^{-1}. Besides the desired high values of heat capacity and enthalpy change during the transition, one more crucial parameter has to be taken into account for the heat storage applications: a long-term reproducibility of the phase change — i.e. the material's stability under thermal stresses. During

accelerated thermal cycle tests it was observed that the samples (two samples with different purities were studied) started to decompose (though slowly) below their published decomposition temperature. The decomposition process seems to be strongly thermally activated and is largely influenced by the upper temperature limit of the heating/cooling cycles. Best results would probably be achieved by cycling at almost isothermal conditions in the close vicinity of the sample melting temperature, which would heavily suppress the decomposition progression.

Acknowledgements

The financial support of the Czech Ministry of Education, Youth and Sports, research projects MSM 0021627501 and LC 523 are gratefully acknowledged. The authors also want to thank doc. P. Šulcová for the TG-DTA measurements.

References

[1] Demirbas M.F.: Energ. Source **1**, 85 (2006).
[2] Kamimoto M.: Thermochim. Acta **41**, 361 (1980).
[3] Cases J.C.: Rev. Chim. Miner. **10**, 577 (1973).
[4] Fokin A., Kumzerov Y., Koroleva E., Naberezhnov A., Smirnov O., Tovar M., Vakhrushev S., Glazman M.: J. Electroceram., DOI 10.1007/s10832-008-9431-4.
[5] Sakiyama M., Kimoto A., Seki S.: J. Phys. Soc. Jpn. **20**, 2180 (1965).
[6] Tanisaki S.: J. Phys. Soc. Jpn. **16**, 579 (1961).
[7] House J.E., Goerne J.M.: Thermochim. Acta **215**, 297 (1993).
[8] Yurtseven H., Caglar I.E.: Spectrochim. Acta A **58**, 55 (2002).
[9] Ema K., Hamano K., Maruyama H.: J. Phys. Soc. Jpn. **57**, 2174 (1988).
[10] Hatta I., Ikushima A.: J. Phys. Chem. Sol. **34**, 57 (1973).
[11] Hatta I., Ichikawa H., Todoki M.: Thermochim. Acta **267**, 83 (1995).
[12] Hoshino S.: J. Phys. Soc. Jpn. **19**, 140 (1964).
[13] Tanisaki S.: J. Phys. Soc. Jpn. **18**, 1181 (1963).
[14] Yamada Y., Shiubya I., Hoshino S.: J. Phys. Soc. Jpn. **18**, 1594 (1963).
[15] Hoshino S., Motegi H.: Jap. J. Appl. Phys. **6**, 708 (1967).
[16] Buchheit W., Herth G., Peterson J.: Solid State Commun. **40**, 411 (1981).
[17] Takase A., Miyakawa K.: J. Phys. C Solid State **18**, 5579 (1985).
[18] Fahim M.A.: Thermochim. Acta **363**, 121 (2000).
[19] Sawada S., Nomura S., Fujii S., Yoshida I.: Phys. Rev. Lett. **1**, 320 (1958).
[20] Hamano K. : J. Phys. Soc. Jpn. **19**, 945 (1964).
[21] Wyncke B., Brehat F., Kozlov G. V.: Phys. Status Solidi B **129**, 531 (1984).
[22] Allen F.H.: Acta Cryst. B **58**, 380 (2002).

[23] O´Neill M.O.: Anal. Chem. **38**, 1331 (1966).
[24] Oza T.M.: J. Indian Chem. Soc. **22**, 173 (1945).
[25] Szper V.J., Fiszmon K.: Z. Anorg. Allg. Chem. **206**, 257 (1932).
[26] Green D.W., Perry R.H.: *Perry's Chemical Engineers' Handbook*, 8th Ed., McGraw-Hill, 2008.